

Original article

Comparison of chest radiography, chest tomosynthesis and computed tomography for detection of pulmonary nodules: A phantom study

Kattipathanapong T,¹ Euathrongchit J,¹ Wannasopha Y,¹ Ua-Apisitwong S,¹ Jirapong K,¹ Saeteng S,² Tantraworasin A² and Lertprasertsuke N³

¹Department of Radiology, ²Department of Surgery, ³Department of Pathology, Faculty of Medicine, Chiang Mai University

Objective To compare the rate of pulmonary nodule detection using chest radiograph, chest digital tomosynthesis and computed tomography examination.

Methods After institutional review board approval, an in-house chest phantom was made from acrylic, plaster and catheters. Plastic beads of 1-2 mm, 3-4 mm, 5-6 mm, 7-8 mm and 9-10 mm were implanted in the phantom to represent pulmonary nodules. From 0 to 20 nodules were randomly embedded in each model and the model was photographed by digital chest radiograph (CXR), chest digital tomosynthesis (CDT) and chest computed tomography (CT). Two blinded thoracic radiologists reviewed and marked the nodules on each of 34 images. The percentage of nodules detected with each method was calculated and compared.

Results There were a total of 332 nodules in the 34 phantom models. Overall nodule detection rates were 75.3% for CXR, 91.0% for CDT and 98.8% for CT. With CT, all nodules larger than 3 mm in diameter were identified. With CDT, over 90% of the nodules larger than 5 mm were detected. The percentage detected with CDT and CT was not statistically significantly different for 5-10 mm nodules. The regions of poorest nodular detection with CXR were the mediastinum and hilum regions, while with CDT it was the costophrenic sulcus.

Conclusion CT provides the highest percentage of nodular detection, followed by CDT and digital CXR in that order. There is no significant difference in percentage detection between CT and CDT for 5-10 mm nodules. **Chiang Mai Medical Journal 2019;58(4):191-8.**

Keywords: chest radiograph, digital tomosynthesis, computed tomography

Introduction

Chest radiography (CXR) is commonly used for evaluating patients with pulmonary disease (1). However, its sensitivity and specificity are quite low because it is limited by overlapping anatomy (2-4). That limitation does not occur with

Computed Tomography (CT). However, CT has the disadvantages of high cost and high radiation dose (5, 6). Recently, a new technique called digital tomosynthesis was developed which can reconstruct sectional images at arbitrary depths

Correspondence: Juntima Euathrongchit, MD., Department of Radiology, Faculty of Medicine, Chiang Mai University, Chiang Mai 50200 Thailand.

E-mail: jeuathro@med.cmu.ac.th

Received: November 8, 2018; **Revised:** April 25, 2019; **Accepted:** May 27, 2019



by collecting a number of projection images at different angles using a digital detector (DT) (7). The amount of overlapping anatomy in the section images with DT is much less than with standard projection radiographs. Many articles have described the benefits of DT (7-9,12,14). There is, however, a learning curve for the interpretation of this new technology. The purpose of this study was to compare the detection rate of nodules using the modalities of CXR, chest digital tomosynthesis (CDT) and CT examination with phantom models prior to clinical application.

Methods

The institutional review board granted permission for this study as an exemption type. Phantom model and study design: Chest phantoms were made using an acrylic plate to represent soft tissue, acrylic bars and angiography-catheters to represent the pulmonary vessels, plaster to represent bone and foam to represent lung parenchyma. The models consisted of 22 sections, each with a slab thickness of 10 mm. Different diameter plastic beads were used to represent lung nodules of different sizes. The plastic beads were divided in to

5 groups: 1-2 mm, 3-4 mm, 5-6 mm, 7-8 mm and 9-10 mm. Figure 1 shows a phantom with plastic nodules and representative images from each scanning modality. A total of 34 phantom models with different sizes and numbers of nodules were created. The number of nodules in each model ranged from none to 20. The nodules' position and size were randomized using a standard random number generator. The CXR, CDT and CT scans of each phantom experiment were all done on the same day.

Imaging techniques: Posteroanterior CXR was performed at 120 kV and 320 mA using digital radiography (Definium 8000; GE Healthcare, Chalfont St. Giles, England.). CDT used Volume RAD software (GE Healthcare) to collect sixty low-dose projection images at a tube voltage of 120 kV within 11 seconds with a fixed detector and continuous vertical movement of the x-ray tube from -17.6 to +17.6 degrees around the standard orthogonal posterior anterior position. Sixty coronal images were obtained with a nominal thickness of 4 mm without overlap. Multidectector CT (MDCT) examinations were performed with a 16-channel scanner (Aquilion 16, Toshiba,

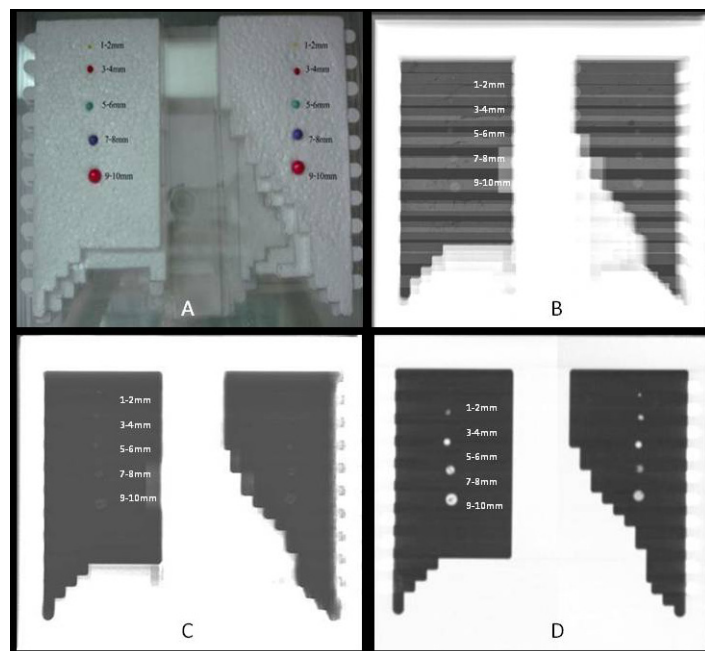


Figure 1. (A) Nodules in the chest phantom; (B) nodules in chest radiograph; (C) nodules in chest digital tomosynthesis image; (D) nodules in CT image

Tochigi-Ken, Japan) following the standard protocol of the author's department. The scan parameters were 120 kV and 180–500 mA; each section thickness and interval was 1.0 mm. Axial and coronal images were reconstructed with a 5 mm thickness and interval. All images were saved using a picture archiving and communication system (CMUPACS, Faculty of Medicine, Chiang Mai University, Chiang Mai Thailand).

Detection Study: Softcopy DICOM images were evaluated on a Panacea workstation (version 2.0.1, Bangkok, Thailand) by two thoracic radiologists, one with 13 years (JE) and one with 2 years of experience (YW), who knew only that there were either none or multiple nodules in each model. They were allowed to adjust window width, window level, pan, and zoom and to mark detected nodules as desired. To avoid recall bias, images were divided into 3 groups based on modality; the order of presentation of the images was randomized using a standard random number generator. Each radiologist independently interpreted CXR, CDT and CT images in that order. Any questionable nodules were discussed by the two radiologists to reach a final agreement. Figure 2 shows detected nodules on images of each modality.

Statistical analysis

Marked nodules from the CXR, CDT and CT images were compared with the actual nodular locations and classified as either detected

or undetected nodules. The percentage of nodules detected with each modality was calculated using SPSS software (SPSS version 16; SPSS, Chicago, Ill). Differences between detection percentages with each modality and differences between the two observers were analyzed by comparison of proportion using MedCalc version 11 (MedCalc Software; Mariakerke, Belgium).

Results

Summaries of the detection of the 332 nodules in the 34 phantom models with each modality are shown in Figures 3 and 4. The overall detection rates were 98.8% with CT, 91% with CDT and 75.3% with CXR. With CT, all nodules larger than 2 mm were detected (100% detection) and 93.7% of the 1-2 mm nodules were detected. CDT detection rates increased with nodule size, from 82.5% for 1-2 mm nodules to 98.3% for 9-10 mm nodules. With CXR, the detection rate was 52.4% for 1-2 mm nodules and 89.8% for 9-10 mm nodules. The detection rate with CT was significantly higher than with CXR; CT showed better nodular detection than CDT only for 3-4 mm nodules (Table 1). Detection rates of all but one of the nodular groups with CDT were significantly higher than with CXR ($p < 0.05$). The exception was 9-10 mm nodules, where the difference was not significant. The locations with lower detection rates on chest radiographs were the hilum and the retrocardiac areas (Figure 5), while a blind area of CDT was the costophrenic sulcus (Figure 6).

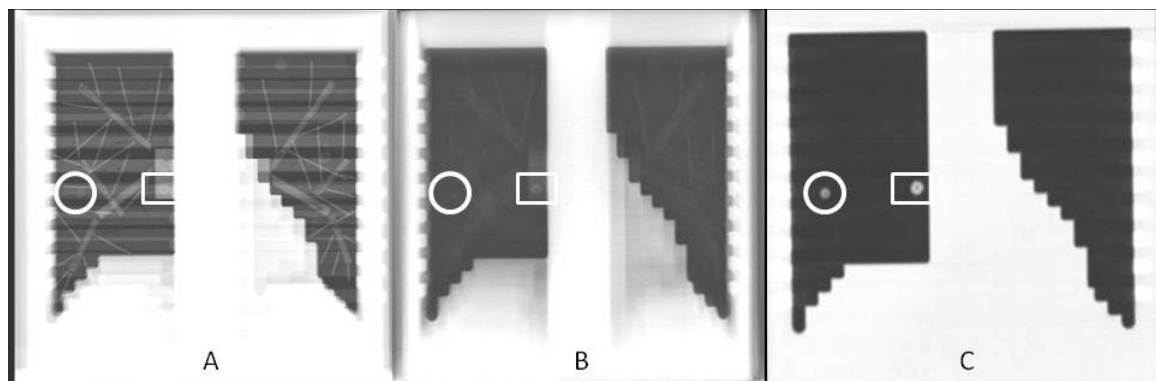


Figure 2. Small nodules as circles and rectangles: (A) chest radiograph; (B) chest digital tomosynthesis; (C) coronal CT – lung window

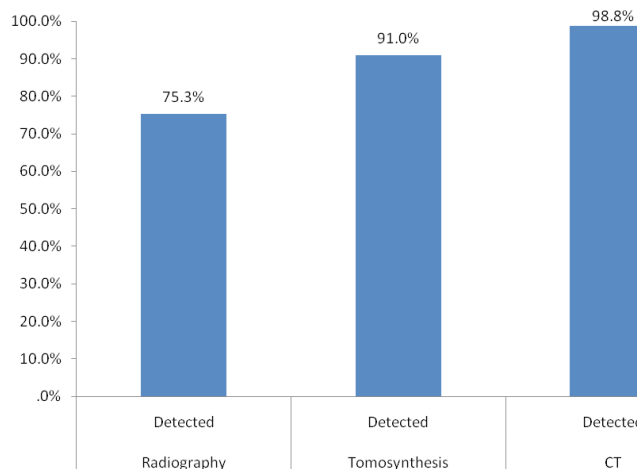


Figure 3. Percentage of nodules detected with each modality

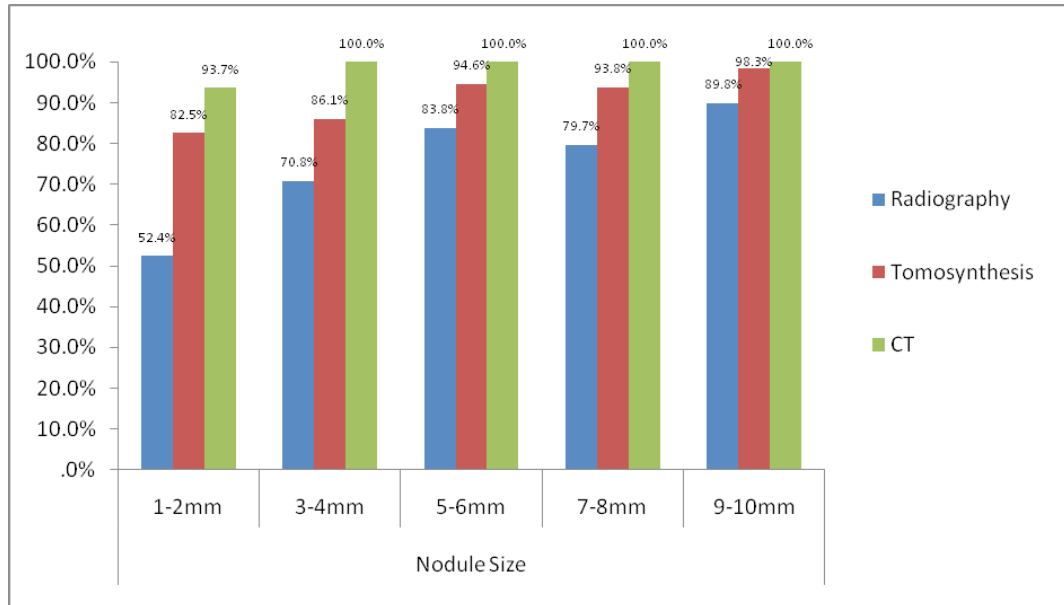


Figure 4. Percentage of nodules detected by modality and nodule size

Table 1. Detection rates with different modalities

Nodule size	Dif(%)	95% CI	p-value	Dif(%)	95% CI	p-value	Dif(%)	95% CI	p-value
1-2 mm	30.10	12.84-45.57%	0.0006*	41.30	25.64-55.05%	< 0.0001*	11.20	-1.20-23.71%	0.0957
3-4 mm	15.30	0.94-29.12%	0.0424*	29.20	17.91-41.1%	< 0.0001*	13.90	5.28-24.08%	0.0032*
5-6 mm	10.80	-0.09-21.91%	0.0641	16.20	7.23-26.59%	0.0009*	5.40	-0.84-13.26%	0.1287
7-8 mm	14.10	1.37-26.83%	0.0364*	20.30	9.68-32.21%	0.0004*	6.20	-0.98-15.17%	0.1301
9-10 mm	8.50	-1.25-19.30%	0.1182	10.20	1.42-20.87%	0.0357*	1.70	-4.58-9.09%	0.9976

Dif; difference ; p; p-value, *significance at $p < 0.0$

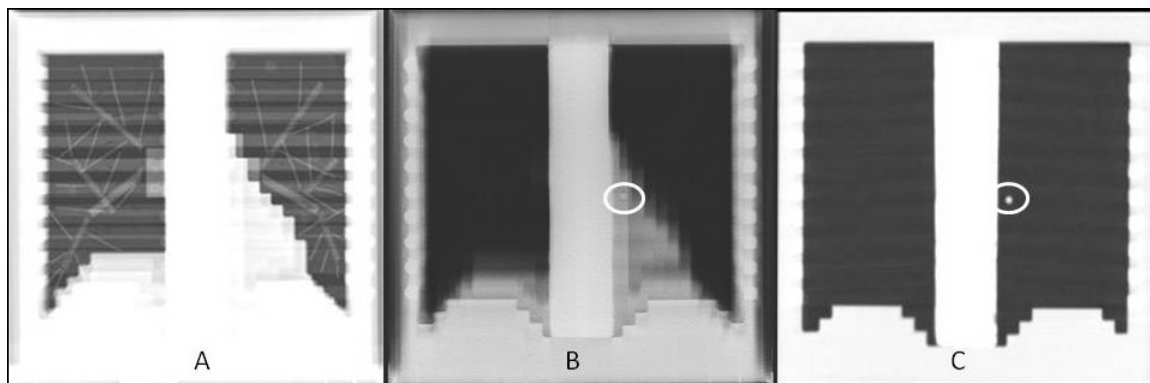


Figure 5. The small nodule was identified on only with chest digital tomosynthesis (B) and coronal CT images – lung window (C) (circles). It was not detected with the chest radiograph (A). The nodules were in the superior retrocardiac region.

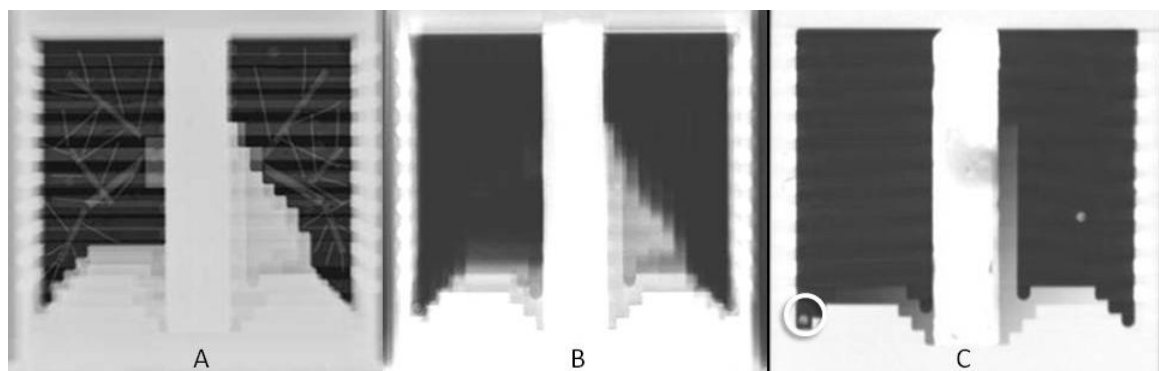


Figure 6. The small nodule in the right costophrenic sulcus (circle) was detected with coronal CT – lung window image (C), but was not with the chest radiograph (A) or the chest digital tomosynthesis image (B).

Agreement rates between the two observers were 94% for CT, 88.3% for CDT and 86.7% for CXR.

Discussion

CXR, since it is available worldwide and easy to perform, is still a key in the diagnosis of many thoracic diseases. In this digital era of rapid technological advances, many techniques, including both hardware and software, are developed with the aim of overcoming the limitations of chest radiographs, e.g., flat-panel detector systems and computed radiographs replacing conventional film, improved visual presentation techniques and soft-copy reading, and automated diagnostic interpretation including computer-aided detection (CAD). New image post-processing techniques include edge enhancement and multifre-

quency processing. Among recent developments in applications to improve interpretation are dual energy subtraction, temporal resolution subtraction and digital tomosynthesis (8).

As treatment of lung cancer in the early stages provides the best benefit, many researchers have actively sought a better early detection screening test. Recently, the use of CT images as a screening test for lung cancer has been approved. However, the cost and radiation dose of CT are both still high. Multiple techniques to improve chest radiographs have also been created, including digital tomosynthesis. Vikgren J, et al. (9) showed that the most effective tomosynthesis dose is 0.12 mSv. That is approximately two times higher than standard PA and lateral examinations (0.06 mSv) (6), but about 30 times lower than CT examina-

tions (4-7 mSV) and about 12 times lower than low dose CT scans (1.5 mSV) (10). Identification of small nodules is important for early detection of lung cancer. The important cutoff point is nodules of about 4 mm diameter (11). This study determined that the overall detection rate with a CT image was the highest, followed by CDT and CXR. There was no statistically significant difference in the detection rate between CT and CDT for nodules 5-6 mm, 7-8 mm and 9-10 mm in diameter. With smaller nodules (1-2 mm and 3-4 mm), the detection rate using a CT scan was better than digital tomosynthesis. In addition, both CT and CDT showed a better detection rate than CXR. Nodules of 1-2 mm were difficult to see with all modalities; CXR revealed only 52.4%, CDT found 82.5% and CT scan detected 93.7%. These findings are similar to a study by Vikgren J, et al. (9) which reported that the difference in detection percentage between CDT and CT was not statistically significant but that CDT and CT both had a higher sensitivity than CXR for detecting nodules smaller than 9 mm. A study by Triphuridet N, et al. reported that the sensitivity of CDT is comparable to low-dose computed tomography (LDCT), particularly for pulmonary lesions larger than 10 mm (12).

Since it takes longer to analyze a CT scan than a CDT scan, it may be cost-effective to search for nodules with CDT before studying the details and morphology of nodules using CT. CDT may also be helpful for follow-up during the treatment period or in searching for lung metastases. Currently, there are many applications of tomosynthesis for various clinical tasks, including angiography, chest imaging, mammography, dental imaging and orthopedic imaging (13-14).

There were some limitations in this study. The in-house simple phantom models lacked the complex bronchovascular markings and the mediastinal structures which frequently obscure lesions in patients. Also, the authors did not directly measure the radiation dose of each modality. As this was the first study using the digital tomosynthesis software at this institution, the protocol used was based on available commer-

cial protocols rather than a protocol designed specifically for the study. It is still necessary to discover and refine specific diagnostic techniques prior to clinical use.

Conclusions

The average overall nodule detection rates with CXR, CDT and CT were 75.3%, 91.0% and 98.8%, respectively. Both CDT and CT have a higher detection rate for small nodules than CXR; that difference is statistically significant for nodules less than 8 mm diameter. There is no statistical difference between CDT and CT detection rates for nodules of 5-10 mm.

Acknowledgements

The authors would like to thank Rochana Phuackchantuck, MSc, for providing statistical advice as well as Akadet Phuyousuk and Narin Plengsai for phantom construction.

References

1. Geitung JT, Skjaerstad LM, Gothlin JH. Clinical utility of chest roentgenograms. *Eur Radiol*. 1999;9:721-3.
2. Bath M, Hakansson M, Borjesson S, Hoeschen C, Tischenko O, Kheddache S, et al. Nodule detection in digital chest radiography: effect of anatomical noise. *Radiat Prot Dosimetry*. 2005;114:109-13.
3. Hakansson M, Bath M, Borjesson S, Kheddache S, Grahn A, Ruschin M, et al. Nodule detection in digital chest radiography: summary of the RADIUS chest trial. *Radiat Prot Dosimetry*. 2005;114:114-20.
4. Kaneko M, Eguchi K, Ohmatsu H, Kakinuma R, Naruke T, Suemasu K, et al. Peripheral lung cancer: screening and detection with low-dose spiral CT versus radiography. *Radiology*. 1996;201:798-802.
5. Mayo JR, Aldrich J, Muller NL. Radiation exposure at chest CT: a statement of the Fleischner Society. *Radiology*. 2003;228:15-21.
6. Stabin MG. Doses from Medical Radiation Sources. [online]. Available at: hps.org/hpspublications/articles/dosesfrommedicalradiation.html. Accessed January 15, 2011.
7. Dobbins JT, 3rd, Godfrey DJ. Digital x-ray tomosynthesis: current state of the art and clinical potential. *Phys Med Biol*. 2003;48:65-106.
8. McAdams HP, Samei E, Dobbins J, 3rd, Tourassi GD, Ravin CE. Recent advances in chest radiography. *Radiology*. 2006;241:663-83.
9. Vikgren J, Zachrisson S, Svalkvist A, Johnsson AA,

Boijsen M, Flinck A, et al. Comparison of chest tomosynthesis and chest radiography for detection of pulmonary nodules: human observer study of clinical cases. *Radiology*. 2008;249:1034-41.

10. ACR. Radiation Exposure in X-ray and CT Examinations. [online]. Available at: www.radiologyinfo.org/en/pdf/sfty_xray.pdf. Accessed February 5, 2011.

11. MacMahon H, Austin JH, Gamsu G, Herold CJ, Jett JR, Naidich DP, et al. Guidelines for management of small pulmonary nodules detected on CT scans: a statement from the Fleischner Society. *Radiology*. 2005;237:395-400.

12. Triphuridet N, Singharuksa S, Sricharunrat T, Screening of lung cancer by low-dose CT(LDCT), digital tomosynthesis (DT) and chest radiography (CR) in a high risk population: A comparison of detection methods. *Journal of Thoracic Oncology*. 2013;S148-9.

13. Dobbins JT, 3rd, McAdams HP. Chest tomosynthesis: technical principles and clinical update. *Eur J Radiol*. 2009;72:244-51.

14. Mermuys K, De Geeter F, Bacher K, Van De Moortele K, Coenegrachts K, Steyaert L, et al. Digital tomosynthesis in the detection of urolithiasis: Diagnostic performance and dosimetry compared with digital radiography with MDCT as the reference standard. *Am J Roentgenol*. 2010;195:161-7.

การเปรียบเทียบระหว่างภาพเอกซเรย์ปอด ภาพเอกซเรย์ชนิดดิจิทัลໂໂມชິນເທີສ ແລະ ภาพเอกซเรย์ຄວມພິວເຕອົວເພື່ອตรวจກ້ອນໃນປອດ ໂດຍທດລອງໃນຫຸ່ນຈຳລອງ

ຮນເນສ ຂັດຕິພັນນາພົງ,¹ ຈັນທິມາ ເອື່ອຕຽງຈິຕີຕີ,¹ ຍຸທຣິພັນນີ້ ວຽຣະໂສກາ,¹ ສຸພຈົນ ເອື່ອກິສິທິງົງກົດ,¹

ເກີຍຣັດພົງ,¹ ຈິຣະພົງ,¹ ສມເຈຣິມ ແຊ່ເຕິງ,² ອົງກາຕີ ຕັນຕິວະຄິລີປ,² ແລະ ນິຮັຊ ເລີສປະເສີງສູງ³

¹ກາງວິຊາຮັງສິວິທີຍາ, ²ກາງວິຊາສ້າລຍະຄາສົດ, ³ກາງວິຊາພາຍາອິວິທີຍາ ຄະນະແພທຍຄາສົດ ມາຮວິທີຍາລ້າຍເຊີງໃໝ່

ວັດຖຸປະສົງດ ເພື່ອຫາວັດທະນາການຕະຫຼາມກ້ອນໃນປອດຈາກການຕະຫຼາມ ເກຊເຮົຍປອດ ເກຊເຮົຍໝັດຕິທັລໂໂມຈິນ
ເທີສ ແລະເກຊເຮົຍຄວມພິວເຕອົວ ຮົມຄົງອັດການຕະຫຼາມຕະຫຼາມເພື່ອປະຫວັງໝັດການຕະຫຼາມຕ່າງໆ

ວິຊີກາຣ ຮັບອັນດາການຮັບອອງຈາກກະນົມການຈິຍຮຽມຈານວິຈີຍ ຫຸ່ນຈຳລອງປອດຈຶ່ງໄດ້ຈັດທຳຈາກແຜ່ນອະຄວິລືກ
ປຸນປາລາສເຕົວໝັງແລະສາຍສາວໝາດລົດເລື່ອດ ກ້ອນໃນປອດທຳຈາກເມື່ອດຳລັບພລາສົດິການນາດ 1-2 ມມ. 3-4 ມມ. 5-6 ມມ. 7-8 ມມ.
ແລະ 9-10 ມມ. ໃສ່ເຂົ້າໄປໃນຫຸ່ນຈຳລອງ ຈຳນວນຕັ້ງແຕ່ 0 ຍື້ 20 ເມັດ ໂດຍການສຸມ ແລ້ວນໍາຫຸ່ນຈຳລອງໄປຄ່າຍກາພ
ດິຈິທັລເກຊເຮົຍປອດ (CXR) ພາບເກຊເຮົຍໝັດຕິທັລໂໂມຈິນເທີສ (CDT) ແລະ ພາບເກຊເຮົຍຄວມພິວເຕອົວ (CT)
ກາພເກຊເຮົຍທີ່ໄດ້ທັງໝົດຈະກູກແປລັດໂດຍ ຮັງສີແພທຍ 2 ດາວ ຜົ່າງຈະກູກປົດບັງຂອມູນທີ່ເກີຍກັບກ້ອນໃນຫຸ່ນຈຳລອງ
ແລະໃຫ້ຮະບຸຕໍາແໜ່ງຂອງກ້ອນໃນແຕ່ລະກາພ ຮັບອັນດາການຕະຫຼາມກ້ອນທີ່ຕະຫຼາມປິບໃນແຕ່ລະ
ການຕະຫຼາມແລະເປົ້າມີການຕະຫຼາມຕ່າງໆ

ຜລກຮັກສົກຂາ ມີກ້ອນຈຳນວນ 332 ກ້ອນໃນຫຸ່ນຈຳລອງ 34 ຫຸ່ນ ອັດການຕະຫຼາມກ້ອນຂອງ CXR CDT ແລະ CT
ຄືວ ຮ້ອຍລະ 75.3 91.0 ແລະ 98.8 ຕາມລຳດັບ ການຕະຫຼາມຕ້ອງ CT ສາມາດຕະຫຼາມຈັບກ້ອນໄດ້ທັງໝົດ ທີ່ມີນາດໃຫຍ່
ກວ່າ 3 ມມ. CDT ສາມາດຕະຫຼາມກ້ອນທີ່ມີນາດມາກວ່າ 5 ມມ. ໄດ້ມາກກວ່າຮ້ອຍລະ 90 ເມື່ອເປົ້າມີການຕະຫຼາມຕ່າງໆ
ຮ້ອຍລະຂອງການຕະຫຼາມກ້ອນທີ່ມີນາດ 5-10 ມມ. ຮະຫວ່າງ CDT ແລະ CT ພບວ່າໄມ່ແຕກຕ່າງອຍ່າງມີນັ້ນສຳຄັນ
ສ່ວນຕຳແໜ່ງກ້ອນໃນທຽບອັກທີ່ຕະຫຼາມປິບໄດ້ໄມ້ດີ ບນກາພ CXR ອູ້ທີ່ໜ້ອງມິດແອສທິນໍ້ມ ແລະ ຂັ້ງປອດ ສ່ວນຂອງກາພ
CDT ອູ້ທີ່ຕຳແໜ່ງຮ່ອງປອດຮ່ວມກັບກະບັງລມ (costophrenic sulcus)

ສຽງ CT ສາມາດຕະຫຼາມກ້ອນໄດ້ໃນຮ້ອຍລະທີ່ສູງສຸດ ຕາມມາດວ່າງວິຊ CDT ແລະ CXR ອ່າງໄກກີ້ຕາມເນື່ອເປົ້າມີການຕະຫຼາມຕ່າງໆ
ວິຊ ອັດການຕະຫຼາມຕ່າງໆຂອງການຕະຫຼາມກ້ອນນາດ 5-10 ມມ. ຮະຫວ່າງວິຊ CT ແລະ CDT ພບວ່າໄມ່ແຕກຕ່າງອຍ່າງມີນັ້ນສຳຄັນ
ເຊີງໃໝ່ເວົ້າສາຣ 2562;58(4):191-8.

ຄໍາສຳຄັນ: ຕິຈິທັລເກຊເຮົຍປອດ ເກຊເຮົຍໝັດຕິໂໂມຈິນເທີສ ແລະ ເກຊເຮົຍຄວມພິວເຕອົວ